BDNF controls neuropsychiatric manifestations via autophagic regulation of p62 and $GABA_A$ receptor trafficking

Toshifumi Tomoda,[1,2,3,*] Akiko Sumitomo,[1,2,3] Yuki Hirota-Tsuyada,[3] Hitoshi Miyachi,[4]

Hyunjung Oh,[1,2] Leon French,[1,2] and Etienne Sibille[1,2,5,*]

[1]Campbell Family Mental Health Research Institute, Centre for Addiction and Mental Health, Toronto, Ontario M5T 1R8, Canada

[2]Departments of Psychiatry, University of Toronto, Toronto, Ontario M5T 1R8, Canada

[3]Department of Research and Drug Discovery, Medical Innovation Center, Kyoto University Graduate School of Medicine, Kyoto 606-8507, Japan

[4]Institute for Virus Research, Kyoto University, Kyoto 606-8507, Japan

[5]Department of Pharmacology and Toxicology, University of Toronto, Toronto, Ontario M5T 1R8, Canada

*Correspondences: ttomoda1@gmail.com (T.T.), Etienne.sibille@camh.ca (E.S.)

Key words: BDNF, p62, $\alpha5GABA_A$ receptor trafficking, autophagy

HIGHLIGHTS

BDNF constitutively promotes autophagy in cortical pyramidal neurons

Reduced BDNF causes elevated p62 expression, leading to lower surface $\alpha5GABA_AR$ presentation

Reducing p62 levels rescues cognition-related behavioral deficits in *Bdnf*+/- mice

Altered corticolimbic gene expression suggests reduced autophagic activity in depression

SUMMARY

Reduced expression levels of brain-derived neurotrophic factor (BDNF) and disturbances of γ-aminobutyric acid (GABA) neurotransmission have been reported in several neuropsychiatric disorders, including major depression. Although we previously showed a causal link between reduced BDNF signaling and deregulated GABA neurotransmission, a mechanistic link between these two pathways remained elusive. Here we show that *Bdnf* heterozygous (*Bdnf*$^{+/-}$) mice have upregulated expression of sequestosome-1/p62, an autophagy-associated stress response protein, in pyramidal neurons of the prefrontal cortex (PFC), causing reduced surface expression of the α5 subunit of $GABA_A$ receptor (α5$GABA_A$R) in the PFC. Accordingly, *Bdnf*$^{+/-}$ mice exhibit behavioral deficits relevant to the PFC dysfunctions, including cognitive inflexibility and sensorimotor gating deficits. Genetically reducing *p62* gene dosage restored α5$GABA_A$R surface expression and rescued the behavioral deficits in *Bdnf* $^{+/-}$ mice. Translating these findings to humans, altered corticolimbic gene expression profiles from subjects with major depression suggest an overall reduction in autophagic activity in depression. Collectively, the current study reveals that p62 dosage control (*i.e.*, autophagy regulation) may serve as a molecular mechanism linking reduced BDNF signaling, GABA deficits, and psychopathology associated with the PFC functional deficits.

INTRODUCTION

Cognitive impairment is a hallmark symptom associated with a range of psychiatric and neurological conditions (Bast et al., 2017; Knight and Baune, 2018), manifesting either as a core symptom of major mental illnesses (*e.g.*, major depressive disorder [MDD], schizophreia), as age-related decline of brain functions, or as a condition comorbid to neurodegenerative and other brain disorders. Pathobiological mechanisms underlying cognitive impairment include deficits in neural plasticity or synaptic functions (Negrón-Oyarzo et al., 2016); however, the diversity of molecular entities and multiple neurotransmitter systems implicated in synaptic function and neuroplasticity have made it difficult to pinpoint relevant central neurobiological events contributing to cognitive dysfunction, and to identify therapeutic targets that can be effectively targeted to alleviate these symptoms.

Translational molecular studies have consistently reported lower expression levels of brain-derived neurotrophic factor (BDNF) in postmortem samples from subjects with MDD (Guilloux et al., 2012; Tripp et al., 2012), schizophrenia (Pillai et al., 2010; Favalli et al., 2012; Islam et al., 2017), and age-related cognitive decline (Calabrese et al., 2013; Oh et al., 2016). BDNF is a member of the neurotrophin family of growth factors (Chao, 2003) which

plays a number of critical roles in the nervous system, including neuronal survival, proliferation, synaptogenesis, neurotransmission, learning, memory, and cognition (Chao et al., 2006; Lu et al., 2014). Animal models with reduced BDNF expression or activity showed disturbances of neurotransmission or neural plasticity, which likely underlie cognitive deficits observed in these models (Dincheva et al., 2012; Lu et al., 2014; Dincheva et al., 2016), suggesting a contribution of this pathway in cognitive symptoms across a range of psychiatric disorders.

BDNF primarily signals through binding to TrkB receptor and its co-receptor, p75/NTR, leading to activation or modulation of downstream signaling molecules (Chao, 2003). BDNF signaling is also regulated at the receptor level. Upon ubiquitination of TrkB and p75/NTR by TRAF6, an E3 ligase, the ubiquitin-binding adaptor protein, sequestosome-1/p62, is recruited to form a protein complex (TrkB/p75/TRAF6/Ubi/p62), which is then trafficked to an appropriate cellular compartment (*e.g.*, the proteasome or lysosome for degradation, the endosome for internalization or recycling), leading to down- or up-regulation of BDNF signaling in a context-dependent manner (Sánchez-Sánchez and Arévalo, 2017). p62 is a critical adaptor protein that integrates multiple cellular processes, including growth factor

signaling, ubiquitin/proteasomal system, and autophagy/lysosomal system. This occurs by interacting with signaling molecules, ubiquitinated proteins, and autophagy-related protein LC3, respectively (Lippai and Lőw, 2014).

We recently reported that p62 regulates levels of the neuronal cell surface expression of γ-aminobutyric acid $(GABA)_A$ receptors through inreraction with $GABA_A$ receptor-associated protein (GABARAP), an adaptor protein implicated in endocytic trafficking of $GABA_A$ receptors (Sumitomo et al., 2018a). In the prefrontal cortex (PFC) of mice heterozygous for *Ulk2*, an autophagy-regulatory gene, p62 protein levels are elevated as a result of attenuated autophagy, leading to sequestration of GABARAP and hence selective downregulation of $GABA_A$ receptors on the pyramidal neuron surface. This likely underlies cognition-related behavioral deficits observed in these mice (Sumitomo et al., 2018a). In additioin, a recent study reported that TrkB is located to the autophagosome and mediates retrograde transport of this organelle in neurons (Kononenko et al., 2017). These lines of evidence led us to hypothesize that BDNF may regulate autophagy and hence p62 protein levels in neurons, which then affect $GABA_A$ receptor surface expression and GABA neurotransmission, thereby regulating cognitive functions in the brain.

Besides BDNF, we and others have consistently demonstrated dysfunctions of GABA neurotransmission in the corticolimbic circuitry of MDD (Guilloux et al., 2012; Northoff and Sibille, 2014; Fee et al., 2017), schizophrenia (Caballero and Tseng, 2016; Hoftman et al., 2017), and age-related cognitive decline (Porges et al., 2017), suggesting central importance of this inhibitory pathway in the pathophysiology of mental illnesses. As a first step to address a possible link between reduced BDNF levels and deregulated GABA neurotransmission, we recently analyzed transcriptome profiles of the orbitofrontal cortex of young vs. aged human subjects. We demonstrated a positive correlation of exprpession of *BDNF* and GABA synaptic genes (Oh et al., 2016). Moreover, blockage of BDNF signaling in the PFC of mice led to reduction in expression of these GABA synaptic genes, demonstrating a causal link between reduced BDNF signaling and deregulated GABA neurotransmission (Oh et al., 2016). Of particular interest was the α5 subunit of $GABA_A$ receptor (α5$GABA_AR$), whose expression was significantly decreased in aged human brains and in mice with reduced BDNF signaling. Because α5$GABA_AR$ is predominantly expressed by pyramidal neurons in the corticolimbic area of the brain and is responsible for cognitive function (Engin et al., 2013), we hypothesize that correlative dysfunctions of BDNF and α5$GABA_AR$ may underlie deficits of cognitive

dimention observed across multiple neuropsychiatric conditions.

In the present study, we first address a new mechanism by which BDNF controls cell surface presentation of α5GABA$_A$R via regulation of p62 expression levels. We next investigate a functional link between BDNF signaling and α5GABA$_A$R surface expression by manipulating p62 expression levels in mice, through evaluation of cognitive inflexibility and sensorimotor gating deficits. These behavioral endophenotypes are relevant to psychiatric manifestations (Kellendonk et al., 2009; Parnaudesu et al., 2013; Swerdlow et al., 2016) and are commonly observed in BDNF mutant mice (Manning et al., 2013; Parikh et al., 2016) and α5GABA$_A$R-deficint mice (Hauser et al., 2005; Engin et al., 2013). Finally, we analyze the relevance of the autophagy regulatory pathway to neuropsychiatric manifestations, using the gene expression profiles of MDD cohorts. We predict that controlling p62 levels may provide a converging point that links reduced BDNF signaling, GABA deficits, and impaired cognition.

RESULTS

BDNF regulates autophagy in cortical neurons

Autophagy is a specialized membrane trafficking machinery and a major cellular recycling system primarily responsible for degrading old proteins and damaged organelles in the lysosome, which ultimately contributes to the maintenance of cellular homeostasis (Mizushima and Komatsu, 2011). Recent studies demonstrated new roles of autophagy in higher-order brain functions, through synapse pruning (Tang et al., 2014) or $GABA_A$ receptor trafficking (Sumitomo et al., 2018a), suggesting that autophagy deficits may serve as pathobiological mechanisms underlying cognition-related behavioral deficits relevant to neuropsychiatric disorders, including autism (Tang et al., 2014) and schizophrenia (Sumitomo et al., 2018a, b).

As a first step to address the role of BDNF in neuronal autophagy, we prepared primary cortical neurons from transgenic mice expressing GFP-LC3, a fluorescent marker for the autophagosome (Mizushima et al., 2004), and cultured them for 16 days before treating them with BDNF (100 ng/ml) for 30 min. We observed an increase in number and size of GFP-LC3-positive punctate structures (**Figure 1A**), suggesting either *de novo* autophagosome formation due to autophagy induction, or the accumulation of LC3 due to attenuated

autophagic degradation. To discriminate between these two possibilities, we performed the autophagy flux assay (Mizushima et al., 2010); BDNF increased the autophagy flux (*i.e.*, the difference between the amount of membrane-bound LC3 (*i.e.*, LC3-II) seen in the presence vs. the absence of lysosomal protease inhibitors, which reflects the amount of LC3 degraded through an autophagy-dependent process within the lysosome) (**Figure 1B**), suggesting that BDNF has an autophagy-inducing activity in cortical neurons.

We next tested whether BDNF could affect the later phase of autophagy (*i.e.*, maturation stage). This can be assessed by evaluating the acidity of the autophagosome/lysosomal system using LysoTracker (Mizushima et al., 2010). To facilitate simultaneous observation of autophagosome formation and maturation, primary cortical neurons prepared from wild-type (WT) mice were transfected with GFP-LC3 and then labeled with LysoTracker for the last 5 min of the culture period, 30 min after adding BDNF in culture. BDNF markedly increased the extent of LysoTracker uptake by the soma (**Figure 1C**), indicating that BDNF enhanced maturation of the autophagy/lysosomal system in neurons. Consistently, neurons with greater levels of LysoTracker uptake exhibited increase in number and size of the autophagosome located to the neurite (**Figure 1C**, arrows). This suggests that BDNF has an

autophagy-promoting activity in cultured cortical neurons.

Reduced BDNF expression leads to elevated p62 levels in cortical pyramidal neurons

To address the endogenous activity of BDNF in the regulation of autophagy *in vivo*, we quantitated the level of p62 protein in the medial prefrontal cortex (mPFC) of *Bdnf*$^{+/-}$ mice. In this brain region, BDNF is predominantly produced by CaMKII-positive pyramidal neurons and functions as an autocrine and paracrine factor to modulate the activity of neighboring excitatory and inhibitory neurons (Tripp et al., 2012). p62 is used as an *in vivo* marker of autophagic activity, because it is the obligatory adaptor protein selectively targeted for autophagic degradation (Mizushima et al., 2010). The results show a significant increase in p62 protein levels in CaMKII-positive neurons of *Bdnf*$^{+/-}$ mice, as compared to WT control mice (**Figure 1D and 1E**). This increase in protein level was not paralleled by an increase in transcriptional activity of the *p62* gene (**Figure 1F**), implying that the increased levels of p62 may result from reduced rates of protein degradation. These results suggest decreased autophagic activity in the presence of reduced BDNF levels, consistent with the idea that BDNF serves as a constitutive factor enhancing autophagy. To obtain further evidence in

support of reuced autophagy in *Bdnf*$^{+/-}$ mice, we quantitated levels of expression of additional genes in this pathway. Expression of several autophagy regulatory genes (*e.g.*, *Lc3*, *Gabarap*, *Ulk2*) remained unchanged, whereas expression of *Ulk1*, a gene critical to autophagy induction (Mizushima and Komatsu, 2011), was significantly downregulated by ~25% (**Figure 1F**). Together the data suggest a mechanism underlying attenuated autophagy in *Bdnf*$^{+/-}$ mice, which results in persistent upregulation of p62 protein expression in the PFC.

Elevated p62 expression in *Bdnf*$^{+/-}$ cortical neurons causes downregulated surface presentation of α5GABA$_A$R

We recently reported that, similar to *Bdnf*$^{+/-}$ mice, p62 protein expression levels are elevated in pyramidal neurons of the PFC in mice with attenuated autophagy, leading to downregulation of neuronal surface expression of GABA$_A$ receptors through sequestration of GABARAP, an adaptor protein responsible for endocytic trafficking of GABA$_A$ receptors (Sumitomo et al., 2018a). Besides, we previously showed that blockage of BDNF signaling in the PFC causes decreased expression of GABA synaptic genes, most notably that of α5GABA$_A$R, a dendritically-targeted subunit of GABA$_A$ receptors predominantly expressed by pyramidal

neurons (Oh et al., 2016). These results suggest a role of BDNF in GABA neurotransmission through regulation of α5GABA$_A$R localization at the dendrites of pyramidal neurons. We therefore reasoned that the elevated p62 expression in *Bdnf*$^{+/-}$ neurons may influence surface presentation of α5GABA$_A$R.

Surface biotinylation of cultured cortical neurons showed that levels of cell surface α5GABA$_A$R expression were reduced in *Bdnf*$^{+/-}$ neurons, as compared with WT control neurons (**Figure 2A**). Notably, reducing the *p62* gene dosage in *Bdnf*$^{+/-}$ neurons, using cortical neurons from *Bdnf*$^{+/-}$;*p62*$^{+/-}$ mice, restored α5GABA$_A$R surface levels to WT levels (**Figure 2A**), suggesting p62 is a critical adaptor mediating BDNF-induced altered trafficking of α5GABA$_A$R.

To validate this finding *in vivo*, we performed receptor cross-linking assays using bis(sulfosuccinimidyl)suberate (BS3), a membrane-impermeable chemical cross-linker (Boudreau et al., 2012). As the cross-linking reaction proceeds in the presence of BS3, only the fraction of receptors expressed on the plasma membrane surface are expected to be covalently cross-linked with anonymous cell surface proteins, thereby transforming into higher molecular weight species, while the rest of the receptors associated with the endomembrane

would remain intact, maintaining their original molecular weights. The PFC from WT and *Bdnf*$^{+/-}$ mice were subjected to the cross-linking reaction for 3 h and the levels of a series of $GABA_AR$ subunits (*i.e.*, α1, α2, and α5) were measured as a function of time. Although the surface levels of α1- or α2-$GABA_AR$ were equivalent between WT and *Bdnf*$^{+/-}$ mice (**Supplemental Figure 1**), those of α5-$GABA_AR$ showed a significant difference (**Figure 2B**). We observed a time-dependent decrease in the levels of intact α5$GABA_AR$ (~50 kDa); specifically ~53% of total α5$GABA_AR$ underwent mobility shift toward a higher molecular weight range during the 3-h assay period (**Figure 2B**, left). By contrast, the PFC from *Bdnf*$^{+/-}$ mice showed a lesser extent (~25%) of decrease in the levels of intact α5$GABA_AR$ during the same assay period, implying reduced levels of surface α5$GABA_AR$ in the PFC of *Bdnf*$^{+/-}$ mice compared to WT mice (**Figure 2B**, middle). The PFC from *Bdnf*$^{+/-}$;*p62*$^{+/-}$ mice showed ~56% of decrease similar to WT, indicating that reducing the *p62* gene dosage restored the surface α5$GABA_AR$ expression to a level equivalent to the WT (**Figure 2B**, right). Thus, decreased BDNF expression results in reduced surface presentation of a specific subunit of $GABA_AR$ (*i.e.*, α5$GABA_AR$) through elevated p62 expression in the PFC.

Elevated p62 expression in *Bdnf*$^{+/-}$ mice causes behavioral deficits relevant to the PFC dysfunction

We then investigated the potential role of elevated p62 expression in PFC-relevant brain functions of *Bdnf*$^{+/-}$ mice, such as information processing and cognition. Previous studies reported that *Bdnf*$^{+/-}$ mice had reduced prepulse inhibition (PPI) of acoustic startle response (Manning et al., 2013), demonstrating a role of BDNF in sensorimotor gating function. This mechanism of filtering sensory information to render appropriate motor responses has been shown to rely in part on the function of the cortical circuitry involving mPFC (Swerdlow et al., 2016). In agreement with the previous study, we confirmed reduced PPI levels in *Bdnf*$^{+/-}$ mice (**Figure 2C**). Reducing the *p62* gene dosage in *Bdnf*$^{+/-}$ mice (*i.e.*, using *Bdnf*$^{+/-}$;*p62*$^{+/-}$ mice) rescued the PPI deficits back to levels observed in control WT mice (**Figure 2C**), together suggesting that decreased expression of BDNF results in sensorimotor gating deficits through elevated p62 expression in the nervous system.

Bdnf$^{+/-}$ mice were also recently shown to have reduced cognitive flexibility in a visual discrimination task (Parikh et al., 2016). To further address deficits in cognitive flexibility in *Bdnf*$^{+/-}$ mice, we used a rule shifting paradigm (Bissonette et al., 2008; Cho et al., 2015), in

which mice were initially trained to associate food reward with a specific stimulus (*i.e.*, either an odor or a digging medium) and subsequently evaluated for cognitive flexibility by changing the type of stimulus that predicts the reward (**Figure 2D**). *Bdnf*$^{+/-}$ and WT mice learned the association rule in a similar number of trials during the initial association phase of trials; however, *Bdnf*$^{+/-}$ mice required significantly higher numbers of trials to shift their behavior during the rule shifting phase of trials (**Figure 2E**). When the *p62* gene dosage was reduced in *Bdnf*$^{+/-}$ mice (*i.e.*, in *Bdnf*$^{+/-}$;*p62*$^{+/-}$), the mice showed cognitive performance indistinguishable from that of controls (**Figure 2E**), together suggesting that decreased expression of BDNF results in cognitive deficits through elevated p62 expression.

Elevated p62 expression is sufficient to cause downregulation of surface α5GABA$_A$R expression and behavioral deficits

To further address the causal role of elevated p62 expression in the regulation of α5GABA$_A$R surface expression and the associated behavioral changes, we generated p62-transgenic (Tg) mice, in which p62 transgene expression was driven by CaMKII promotor. Among three Tg lines established, two lines (#1, #3) showed ~60% increase in the level of p62 protein

expression in the PFC, while one line (#2) failed to overexpress p62 as evaluated by Western blot (**Figure 3A**). BS3 cross-linking assays demonstrated that the PFC of the p62-Tg line (#1) had reduced levels of surface $\alpha5GABA_AR$ expression compared to WT, whereas non-overexpressing line #2 had surface $\alpha5GABA_AR$ expression equivalent to the WT (**Figure 3B**).

We next evaluated sensorimotor gating in the p62-Tg lines. p62-Tg lines (#1, #3) exhibited reduced levels of PPI, whereas the non-overexpressing line #2 had PPI levels that were not different from WT levels (**Figure 3C**). We then assessed cognitive flexibility. p62-Tg mice (#1, #3) learned the association rule during the initial association phase of trials in a similar manner as WT; however, the two lines were impaired during the rule shifting phase of trials (**Figure 3D**).

Together these data demonstrated that elevated p62 levels in CaMKII-expressing pyramidal neurons in the PFC and corticolimbic areas are sufficient to replicate the molecular and behavioral phenotypes of *Bdnf*$^{+/-}$ mice; specifically, reduced surface expression of $\alpha5GABA_AR$ and PFC-relevant behavioral deficits.

Gene expression profiling suggests altered autophagy machinery in the brain of MDD subjects

Although reduced levels of expression and/or functioning of BDNF and α5GABA$_A$R are consistently reported in the brains of several neuropsychiatric conditions (Guilloux et al., 2012; Oh et al., 2016; Fee et al., 2017), including MDD, the cellular machinery that may underlie these changes remains to be understood. On the basis of our recent reports showing attenuated neuronal autophagy in several mouse models for neuropsychiatric disorders such as schizophrenia (Sumitomo et al., 2018a, b), as well as our present data demonstrating elevated p62 levels in *Bdnf*$^{+/-}$ mouse model, we hypothesized that alteration in autophagy machinery may contribute to cellular deficits present in MDD.

To test this hypothesis, we analyzed genome-wide differential expression statistics from a meta-analysis of 51 MDD patients and 50 controls (Ding et al., 2015). This study combined 8 independent microarray datasets that profiled expression in corticolimbic areas. Autophagy-related genes were defined by gene ontology (GO) (Huang et al., 2009; Huang et al., 2015), and combined into "autophagy-enhancing" and "autophagy-attenuating" gene lists (See details in **Supplemental Methods** and **Supplemental Tables 1** and **2**). Within the 95

genes included in the “autophagy-enhancing” gene list, 1 gene showed a significant increase ($p<0.05$) compared to the control cohorts, whereas 8 genes showed a significant decrease ($p<0.05$) (**Supplemental Table 1**). By contrast, within the 38 genes included in the “autophagy-attenuating” gene list, 3 genes showed a significant increase compared to the control cohorts, whereas 1 gene showed a significant decrease (**Supplemental Table 2**). When the differential expression summary statistics of the autophagy-enhancing genes (as represented by the area under the curve [AUC] = 0.44) were compared to the autophagy-attenuating genes (AUC = 0.60), a significant difference was observed between these two groups ($p<0.01$) (**Figure 4A**), with the former being slightly enriched for downregulation, whereas the latter was enriched for upregulation in the MDD brain (**Figure 4B**). The data imply that overall activity of autophagy machinery in MDD is shifted toward the direction of downregulation at the transcriptome level.

DISCUSSION

We previously showed that reduced BDNF expression in the PFC causes selective attenuation of GABAergic inhibitory neurotransmission through transcriptional control of GABA-related genes (Oh et al., 2016). In the present study, we demonstrated an additional layer of mechanism by which reduced BDNF signaling negatively impacts GABA functions via control of $GABA_A$ receptor trafficking. Specifically, our data suggest for the first time that dosage control of p62, a molecule implicated in autophagic control of cellular function, provides a key molecular event that links BDNF signaling, GABAergic neurotransmission, and cognitive and other behavioral outcomes relevant to PFC functions.

Neuropsychiatric diseases occur through a complex interaction of multiple genetic and environmental risk factors; the latter includes chronic psychosocial stress in the case of MDD (Fee et al., 2017), and BDNF was identified as a protein downregulated in response to such psychosocial stresses (Guilloux et al., 2012; Tripp et al., 2012). In addition, we have demonstrated that reduced BDNF activity in PFC pyramidal neurons leads to reduced expression levels of presynaptic genes (*e.g.*, *Gad1*, *SLC32A1*) and of neuropeptide genes (*e.g.*, *SST*, *neuropeptide Y*, *cortistatin*) expressed in neighboring inhibitory neurons (Oh et al., 2016),

together suggesting a paracrine mode of BDNF action responsible for attenuated GABA signaling (**Figure 5**, right). Moreover, expression levels of *Gabra5*, a gene encoding α5GABA$_A$R that is predominantly targeted to the dendritic compartment of pyramidal neurons, were among the most significantly downregulated, suggesting an autocrine mode of BDNF action contributing to reduced expression of GABA-related genes. Both modes of transcriptional mechanisms, coupled with the attenuated GABA$_A$ receptor trafficking demonstrated in the current study (**Figure 5**, left), are expected to synergistically reduce GABA neurotransmission across pre- and post-synaptic compartments.

p62 was originally identified as a protein induced by cellular stress condition, and subsequently shown to function as an adaptor protein that integrates multiple cellular processes, including the autophagy/lysosomal pathway (Lippai and Lőw, 2014). Autophagy is activated in response to a range of cellular stresses (*e.g.*, depletion of nutrients and energy, misfolded protein accumulation, oxidative stress) and mitigates such stresses to maintain cellular homeostasis (Mizushima and Komatsu, 2011). Using genetic mouse and cell models, the present study, as well as our recent report (Sumitomo et al., 2018a), demonstrated that autophagy can also control cell-to-cell signaling through regulation of surface expression of

receptors mediating chemical inhibition. Thus, autophagy has the potential to serve as a cellular machinery to adapt to cellular stresses elicited by psychosocial insults. The gene expression data obtained from the brains of human subjects further suggests that the overall activity of the autophagy machinery is attenuated in MDD, which likely contributes to circuitry disturbances through elevated p62 expression and hence downmodulated $GABA_A$ receptor trafficking.

Cognitive function is primarily controlled via the corticolimbic mechanisms, in part through regulation of excitatory and inhibitory neurotransmission (Kellendonk et al., 2009; Caballero and Tseng, 2016). A number of synaptic genes have been implicated in this process, including BDNF and $\alpha5GABA_AR$. Deficits in expression or activity of these genes result in altered GABAergic inhibition, consistent with *Bdnf*$^{+/-}$ mice exhibiting reduced amplitude and frequency of miniature currents (mIPSC) in cortical and thalamic neurons (Laudes et al., 2012). These signaling disturbances in the cortical circuitry are thought to underlie behavioural deficits, such as cognitive inflexibility and sensorimotor gating deficits observed in *Bdnf*$^{+/-}$ mice. Likewise, mice deficient for $\alpha5GABA_AR$ also exhibit cognitive inflexibility (Engin et al., 2013) and sensorimotor gating deficits (Hauser et al., 2005).

There are several limitations to our interpretation of the results. First, given multifaceted roles and multiple binding partners of p62 adaptor protein, it is unlikely that α5GABA$_A$R is the only receptor system or the cellular target afflicted by elevated expression of p62. Additional subunits of GABA$_A$ receptors or cellular machineries may fully explain behavioral deficits observed in *Bdnf*$^{+/-}$ mice. Second, on the basis of predominant expression of BDNF in pyramidal neurons in the PFC or rather restricted expression of α5GABA$_A$R in corticolimbic brain regions, we primarily focused our analysis on the PFC-related molecular and behavioral deficits in the current study. However, more restricted, cell type-specific or brain-region specific manipulation of pathways may be necessary to determine the precise role of these molecules.

Nonetheless, given the critical role of p62 in regulating α5GABA$_A$R trafficking and behavioral outcomes in *Bdnf*$^{+/-}$ mice, we propose that these molecular players (*i.e.*, p62, BDNF, α5GABA$_A$R) critically contribute to cognitive dimensions and other brain functions under both normal and pathophysiological conditions. For instance, p62 protein levels typically increase with age, reflecting a gradual decrease in cellular autophagic activity (Vilchez et al., 2014), and elevated p62 levels or increase in p62$^+$ inclusions are the cardinal features of

neurodegenerative disorders, including Alzheimer's disease and Parkinson's disease (Ferrer et al., 2011; Salminen et al., 2012). Hence, controlling the dosage of p62 protein may provide a potential target for therapeutic intervention against symptoms shared among these disorders, such as cognitive impairment, through augmentation of inhibitory neurotransmission. In particular, surface availability of $GABA_A$ receptors represents a rate-limiting step for GABAergic neurotransmission. Therefore, the mechanisms for regulating surface presentation of $GABA_A$ receptor through p62 dosage control may provide an alternative therapeutic approach for those who do not respond to current treatment of MDD or other neuropsychiatric disorders.

MATERIALS AND METHODS

Animals

Bdnf knockout mice (*Bdnf* ^{tm1Jae}/J, stock No. 002266) were obtained from The Jackson Laboratory (Bar Harbor, USA). GFP-LC3 transgenic mice were provided by Dr. Noboru Mizushima (University of Tokyo, Japan). p62 knockout mice were provided by Dr. Toru Yanagawa (University of Tsukuba, Japan). CaMKII-p62 transgenic mice were generated according to the standard procedures (Nagy et al., 2003). Mice were maintained on the C57BL/6J genetic background for at least 10 generations. Eight to 12-week old male mice were used for behavioral analysis. Behavioral experiments and data collection were performed by the experimenters who were blinded to animal genotypes. Maintenance of mouse colonies and experiments using mice were in accordance with the NIH Guide for the Care and Use of Laboratory Animals, and approved by the Institutional Animal Care and Use Committee at Kyoto University and at the Centre for Addiction and Mental Health affiliated with University of Toronto.

Prepulse inhibition

The startle response and prepulse inhibition (PPI) were measured using a startle reflex measurement system (SR-LAB) as described (Takahashi et al., 2011), with minor modifications. The test session began by placing a male mouse in a plastic cylinder and leaving it undisturbed for 30 min. The background white noise level in the chamber was 70 dB. A prepulse−pulse trial started with a 50-ms null period, followed by a 20-ms prepulse white noise (74, 78, 82, 86, or 90 dB). After a 100-ms delay, the startle stimulus (a 40-ms, 120 dB white noise) was presented, followed by a 290-ms recording time. The total duration of each trial was 500 ms. A test session consisted of six trial types (pulse-only trial, and five types of prepulse−pulse trial). Six blocks of the six trial types were presented in a pseudo-randomized order such that each trial type was presented once within a block. The formula 100−((Response on acoustic prepulse−pulse stimulus trials/Startle response on pulse-only trials) x 100) was used to calculate %PPI.

Rule shift assay

Cognitive flexibility was evaluated in the rule-shifting assay, essentially as described (Bissonette et al., 2008; Cho et al., 2015). In brief, mice were habituated to food, feeding

apparatus, different odor cues and digging medium texture cues prior to testing, and then food-deprived a day before the assays. Mice were initially trained in a sequence of trials to associate a food reward with a specific stimulus (*i.e.*, either an odor or a digging medium). A varying combination of stimulus and food reward was presented to mice per trial. Eight consecutive correct responses to the food reward were considered reaching criterion (*i.e.*, successful establishment of association between the stimulus and the food reward), and the number of trials to reach criterion were scored for each mouse tested before and after rule shifting (*e.g.*, from an odor cue to a different texture cue to predict reward). Upon rule shifting, numbers of errors due to perseveration to an old rule were scored before reaching new criterion.

Quantitative reverse transcription-polymerase chain reaction (qRT-PCR)

Total RNA was extracted from the ACC using RNeasy Mini kit (Qiagen), and reverse-transcribed with a ReverTra Ace cDNA synthesis kit (Toyobo). TaqMan probes were purchased from Applied Biosystems, Inc. All data were normalized with *Gapdh* as reference.

Primary cortical neuron culture

Primary cortical neurons were prepared from E13.5 frontal cortex through papain treatment (0.5 μg/ml in Earle's balanced salt solution supplemented with 5 mM EDTA and 200 μM L-cysteine), followed by mechanical trituration using fire-bore glass pipettes, and plated on poly-D-lysine-coated glass cover slips or glass-bottom dishes (MatTek). The cultures were recovered in serum-containing media (Neurobasal media supplemented with 10% horse serum, 5% fetal bovine serum, and 2 mM glutamine [Gibco]) for 4 h and maintained in serum-free media (Neurobasal media supplemented with B-27 (1:50 diluted), 2 mM glutamine, 50 I.U./ml penicillin, and 50 μg/ml streptomycin), with half of media being replaced with fresh media every 2−3 days. The cultures were used for immunofluorescence analysis or for surface biotinylation followed by Western blot analysis.

Immunofluorescence analysis

Primary cortical neurons cultured for 18–25 days were transfected with GFP-LC3 expression plasmid using Lipofectamine 2000 (Invitrogen) via the standard procedure, and 48 h post-transfection, the cells were incubated with BDNF (Sigma, 100 ng/ml) for up to 40 min

before fixation with 4% paraformaldehyde (PFA) in PBS. When appropriate, LysoTracker (Invitrogen) was included in culture media for the last 5 min of culture period before fixation. Fluorescence images were acquired by confocal microscopy (SP8, Leica) and the fluorescence intensities of GFP+ puncta and LysoTracker uptake were evaluated by ImageJ (NIH).

Surface biotinylation

Biotinylation of cell surface proteins was performed in primary neuron cultures using the cell surface protein isolation kit (Pierce) according to the manufacturer's protocol. Briefly, cells were incubated with ice-cold PBS containing Sulfo-NHS-SS-Biotin (Pierce) for 30 min with gentle rocking at 4°C. Cells were then lysed and precipitated with NeutrAvidin beads. Precipitated proteins were eluted from the NeutrAvidin beads with loading buffer containing dithiothreitol (DTT) and heated for 5 min at 95°C and then analyzed by Western blot.

Chemical cross-linking assay

Cell surface receptor cross-linking assays were performed as described (Boudreau et al., 2012). In brief, mice were decapitated and the coronal brain slices (~1 mm thick) were quickly

prepared using Brain Matrix (Ted Pella) within 30 sec on ice. The prefrontal cortex was then excised from the slices, minced into pieces using a razor blade, and incubated in artificial CSF buffer containing bis(sulfosuccinimidyl)suberate (BS3) cross-linker (2 mM, ThermoFisher) for 30 min to 4 h at 4°C with constant invert mixing. After quenching the crosslinking reaction by adding glycine (100 mM) for 10 min at 4°C, the tissues were harvested by centrifugation (20,000 *g*, 4°C, 2 min). The proteins were prepared in lysis buffer containing 0.1 % Nonidet P-40 (v/v), protease inhibitor and phosphatase inhibitor cocktail, and 1 mM DTT, and analyzed by Western blot.

Western blots

Western blot analysis was performed according to the standard procedure. The primary antibodies used were anti-$GABA_A$ receptor α5 subunit (rabbit, 1:1,000, R&D Systems), anti-NR1 (rabbit monoclonal [1.17.2.6], 1:1,000, Millipore), anti-p62 (guinea pig, 1:1,000, MBL), anti-LC3B (rabbit, 1:1,000, Novus), anti-GAPDH (mouse, 1:1,000, abcam), and anti-α-Tubulin (mouse monoclonal [B-5-1-2], 1:8,000, Sigma).

Immunohistochemistry

For immunohistochemistry analysis, brains of perfused mice (n = 4 per group) were serially cut into 50 μm-thick coronal sections using vibratome (VT1200S, Leica), and the sections from one cohort of mice (a littermate pair of wild-type and *Bdnf*$^{+/-}$ mice) were permeabilized in PBS containing 0.05% Triton X-100 for 1 h, and incubated for 30 min at room temperature in 10% goat serum (Chemicon) in PBS, and simultaneously immunostained for 16 h at 4°C with primary antibodies followed by Alexa Fluor® 488- or 546-conjugated secondary antibodies (Molecular Probes) for 1 h at room temperature. The stained samples were observed using a confocal microscope (SP8, Leica; 40x objective lens, NA = 1.3); images of one optical section (1 μm thick) were acquired from 3 to 6 non-overlapping areas per section, randomly chosen in each brain region (prefrontal cortex), and 3 to 4 serial sections were analyzed. The fluorescence intensities of p62 immunostaining were measured from each neuronal soma (30~50 somas per section) using ImageJ (NIH), with the background levels of staining in adjacent regions being subtracted, and the average immunofluorescence intensity was calculated across all serial sections from every mouse used. The primary antibodies used were: anti-p62 (guinea pig, 1:400, MBL) and anti-CaMKIIα (mouse monoclonal [6G9], 1:500,

Stressmarq).

Human transcriptome analysis

Data from a prior meta-analysis of altered gene expression in MDD was used (Ding et al., 2015). In brief, human postmortem brain samples were obtained after consent from next of kin during autopsies conducted at the Allegheny County Medical Examiner's Office (Pittsburg, PA, USA) using procedures approved by the Institutional Review Board and Committee for Oversight of Research Involving the Dead at the University of Pittsburgh. A total of 51 MDD and 50 control subjects were included in the 8 studies in that report. Samples from the dorsolateral prefrontal cortex (dlPFC), subgenual anterior cingulate cortex (sgACC) or rostral amygdala enriched in lateral, basolateral and basomedial nuclei had been previously collected and processed on Affymetrix HG-U133 Plus 2 or Illumina HT12 gene arrays. Four studies were performed in the sgACC, 2 studies in the amygdala and 2 in the dlPFC. Half of the studies had been performed in female subjects in each brain region. See details on subjects, areas investigated and other parameters in Ding et al., 2015. Differential summary statistics were used to rank the 10,621 genes from the up-regulated gene with the lowest p-value to the

down-regulated gene with lowest p-value. The receiver operating characteristic curve analysis was used to test enrichment of the autophagy-associated gene lists. Significance between the area under the curve (AUC) values for the autophagy-enhancing and autophagy-attenuating gene lists was empirically determined (10,000 comparisons of randomly selected gene sets of the same sizes).

Statistical analysis

All data were represented as mean ± standard error of the mean (SEM) and were analyzed by Kruskal-Wallis test followed by Dunn's multiple comparison test, unless otherwise noted. Behavioral assay data were analyzed by one-way or two-way analysis of variance (ANOVA) followed by Bonferroni post-hoc test, using Prism statistics software (GraphPad). Statistical significance in figures: $*p < 0.05$, $**p < 0.01$.

ACKNOWLEDGMENTS

We thank Dr. Albert Wong for permission to use the startle chamber. This work was supported by grants from the National Institutes of Health (MH-093723 to E.S.), Campbell Family Mental Health Research Institute (to E.S.), and Department of Defense/Congressionally Directed Medical Research Program (W81XWH-11-1-0269 to T.T.).

CONFLICTS OF INTEREST

The authors declare no conflicts of interest.

AUTHOR CONTRIBUTIONS

T.T., A.S., and Y.H.-T. carried out experiments; H.M. generated CaMKII-p62 transgenic mice; H.O. provided analytical tools; L.F. analyzed differential expression summary statistics; T.T. and E.S. wrote and edited the paper.

REFERENCES

Bast, T., Pezze, M., and McGarrity, S. (2017). Cognitive deficits caused by prefrontal cortical and hippocampal neural disinhibition. Br. J. Pharmacol. *174*, 3211–3225.

Bissonette, G.B., Martins, G.J., Franz, T.M., Harper, E.S., Schoenbaum, G., and Powell, E.M. (2008). Double dissociation of the effects of medial and orbital prefrontal cortical lesions on attentional and affective shifts in mice. J. Neurosci. *28*, 11124–11130.

Boudreau, A.C., Milovanovic, M., Conrad, K.L., Nelson, C., Ferrario, C.R., and Wolf, M.E. (2012). A protein crosslinking assay for measuring cell surface expression of glutamate receptor subunits in the rodent brain after in vivo treatments. Curr. Protoc. Neurosci. CHAPTER: Unit–*5*.3019.

Caballero, A., and Tseng, K.Y. (2016). GABAergic function as a limiting factor for prefrontal maturation during adolescence. Trends Neurosci. *39*, 441–448.

Calabrese, F., Guidotti, G., Racagni, G., and Riva, M.A. (2013). Reduced neuroplasticity in aged rats: a role for the neurotrophin brain-derived neurotrophic factor. Neurobiol. Aging *34*, 2768–2776.

Chao, M.V. (2003). Neurotrophins and their receptors: a convergence point for many signalling pathways. Nat. Rev. Neurosci. *4*, 299–309.

Chao, M.V., Rajagopal, R., and Lee, F.S. (2006). Neurotrophin signalling in health and disease. Clin. Sci. (Lond) *110*, 167–173.

Cho, K.K., Hoch, R., Lee, A.T., Patel, T., Rubenstein, J.L., and Sohal, V.S. (2015). Gamma rhythms link prefrontal interneuron dysfunction with cognitive inflexibility in Dlx5/6$^{+/-}$ mice. Neuron *85*, 1332–1343.

Dincheva, I., Glatt, C.E., and Lee, F.S. (2012). Impact of the BDNF Val66Met polymorphism on cognition: implications for behavioral genetics. Neuroscientist *18*, 439–451.

Dincheva, I., Lynch, N.B., and Lee, F.S. (2016). The role of BDNF in the development of fear learning. Depress. Anxiety *33*, 907–916.

Ding, Y., Chang, L.C., Wang, X., Guilloux, J.P., Parrish, J., Oh, H., French, B.J., Lewis, D.A., Tseng, G.C., and Sibille, E. (2015). Molecular and genetic characterization of depression: overlap with other psychiatric disorders and aging. Mol. Neuropsychiatry *1*, 1–12.

Engin, E., Zarnowska, E.D., Sigal, M., Keist, R., Zeller, A., Pearce, R.A., and Rudolph, U. (2013). Alpha5-containing GABAA receptors in dentate gyrus enable cognitive flexibility. FASEB J. *27*, 661.7–661.7.

Favalli, G., Li, J., Belmonte-de-Abreu, P., Wong, A.H., and Daskalakis, Z.J. (2012). The role of BDNF in the pathophysiology and treatment of schizophrenia. J. Psychiatr. Res. *46*, 1–11.

Fee, C., Banasr, M., and Sibille, E. (2017). Somatostatin-positive gamma-aminobutyric acid interneuron deficits in depression: cortical microcircuit and therapeutic perspectives. Biol. Psychiatry *82*, 549–559.

Ferrer, I., Martinez, A., Blanco, R., Dalfó, E., and Carmona, M. (2011). Neuropathology of sporadic Parkinson disease before the appearance of parkinsonism: preclinical Parkinson disease. J. Neural Transm. (Vienna) *118*, 821–839.

Guilloux, J.P., Douillard-Guilloux, G., Kota, R., Wang, X., Gardier, A.M., Martinowich, K., Tseng, G.C., Lewis, D.A., and Sibille, E. (2012). Molecular evidence for BDNF- and GABA-related dysfunctions in the amygdala of female subjects with major depression. Mol. Psychiatry *17*, 1130–1142.

Hauser, J., Rudolph, U., Keist, R., Möhler, H., Feldon, J., and Yee, B.K. (2005). Hippocampal alpha5 subunit-containing GABAA receptors modulate the expression of prepulse inhibition. Mol. Psychiatry *10*, 201–207.

Hoftman, G.D., Datta, D., and Lewis, D.A. (2017). Layer 3 Excitatory and inhibitory circuitry in the prefrontal cortex: developmental trajectories and alterations in schizophrenia. Biol. Psychiatry *81*, 862–873.

Huang, D.W., Sherman, B.T., and Lempicki, R.A. (2009). Systematic and integrative analysis of large gene lists using DAVID Bioinformatics Resources. Nat. Protoc. *4*, 44–57.

Huang, D.W., Sherman, B.T., and Lempicki, R.A. (2009). Bioinformatics enrichment tools: paths toward the comprehensive functional analysis of large gene lists. Nucleic Acids Res. *37*, 1–13.

Islam, F., Mulsant, B.H., Voineskos, A.N., and Rajji, T.K. (2017). Brain-derived neurotrophic factor expression in individuals with schizophrenia and healthy aging: testing the accelerated aging hypothesis of schizophrenia. Curr. Psychiatry Rep. *19*, 36.

Kellendonk, C., Simpson, E.H., and Kandel, E.R. (2009). Modeling cognitive endophenotypes of schizophrenia in mice. Trends Neurosci. *32*, 347–358.

Knight, M.J., and Baune, B.T. (2018). Cognitive dysfunction in major depressive disorder. Curr. Opin. Psychiatry *31*, 26–31.

Kononenko, N.L., Claßen, G.A., Kuijpers, M., Puchkov, D., Maritzen, T., Tempes, A., Malik, A.R., Skalecka, A., Bera, S., Jaworski, J., and Haucke, V. Retrograde transport of TrkB-containing autophagosomes via the adaptor AP-2 mediates neuronal complexity and prevents neurodegeneration. Nat. Commun. *8*, 14819.

Laudes, T., Meis, S., Munsch, T., and Lessmann, V. (2012). Impaired transmission at corticothalamic excitatory inputs and intrathalamic GABAergic synapses in the ventrobasal thalamus of heterozygous BDNF knockout mice. Neuroscience *222*, 215–227.

Lippai, M., and Lőw, P. (2014). The role of the selective adaptor p62 and ubiquitin-like proteins in autophagy. Biomed. Res. Int. *2014*, 832704.

Lu, B., Nagappan, G., and Lu, Y. (2014). BDNF and synaptic plasticity, cognitive function, and dysfunction. Handb. Exp. Pharmacol. *220*, 223–250.

Maciag, D., Hughes, J., O'Dwyer, G., Pride, Y., Stockmeier, C.A., Sanacora, G., and Rajkowska, G. (2010). Reduced density of calbindin immunoreactive GABAergic neurons in the occipital cortex in major depression: relevance to neuroimaging studies. Biol. Psychiatry *67*, 465–470.

Manning, E.E., and van den Buuse, M. (2013). BDNF deficiency and young-adult methamphetamine induce sex-specific effects on prepulse inhibition regulation. Front. Cell. Neurosci. *7*, 92.

Mizushima, N., Yamamoto, A., Matsui, M., Yoshimori, T., and Ohsumi, Y. (2004). In vivo analysis of autophagy in response to nutrient starvation using transgenic mice expressing a fluorescent autophagosome marker. Mol. Biol. Cell *15*, 1101–1111.

Mizushima, N., Yoshimori, T., and Levine, B. (2010). Methods in mammalian autophagy research. Cell *140*, 313–326.

Mizushima, N., and Komatsu, M. (2011). Autophagy: renovation of cells and tissues. Cell *147*, 728–741.

Nagy, A., Gertsenstein, M., Vintersten, K., and Behringer, R. (2003). Manipulating the mouse embryo. A Laboratory Manual. 3rd Edition. Cold Spring Harbor Laboratory Press.

Negrón-Oyarzo, I., Aboitiz, F., and Fuentealba, P. (2016). Impaired functional connectivity in the prefrontal cortex: a mechanism for chronic stress-induced neuropsychiatric disorders. Neural Plast. *2016*, 7539065.

Northoff, G., and Sibille, E. (2014). Cortical GABA neurons and self-focus in depression: a model linking cellular, biochemical and neural network findings. Mol. Psychiatry *19*, 959.

Oh, H., Lewis, D.A., and Sibille, E. (2016). The role of BDNF in age-dependent changes of excitatory and inhibitory synaptic markers in the human prefrontal cortex. Neuropsychopharmacology *41*, 3080–3091.

Parikh, V., Naughton, S.X., Yegla, B., and Guzman, D.M. (2016). Impact of partial dopamine depletion on cognitive flexibility in BDNF heterozygous mice. Psychopharmacol. (Berl) *233*, 1361–1375.

Parnaudeau, S., O'Neill, P.K., Bolkan, S.S., Ward, R.D., Abbas, A.I., Roth, B.L., Balsam, P.D., Gordon, J.A., and Kellendonk, C. (2013). Inhibition of mediodorsal thalamus disrupts thalamofrontal connectivity and cognition. Neuron *77*, 1151–1162.

Pillai, A., Kale, A., Joshi, S., Naphade, N., Raju, M.S., Nasrallah, H., and Mahadik, S.P. (2010). Decreased BDNF levels in CSF of drug-naive first-episode psychotic subjects: correlation with plasma BDNF and psychopathology. Int. J. Neuropsychopharmacol. *13*, 535–539.

Porges, E.C., Woods, A.J., Edden, R.A., Puts, N.A., Harris, A.D., Chen, H., Garcia, A.M., Seider, T.R., Lamb, D.G., Williamson, J.B., and Cohen, R.A. (2017). Frontal gamma-aminobutyric acid concentrations are associated with cognitive performance in older adults. Biol. Psychiatry Cogn. Neurosci. Neuroimaging *2*, 38–44.

Salminen, A., Kaarniranta, K., Haapasalo, A., Hiltunen, M., Soininen, H., and Alafuzoff, I. (2012). Emerging role of p62/sequestosome-1 in the pathogenesis of Alzheimer's disease. Prog. Neurobiol. *96*, 87–95.

Sánchez-Sánchez, J., and Arévalo, J.C. (2017). A review on ubiquitination of neurotrophin receptors: facts and perspectives. Int. J. Mol. Sci. *18*, pii: E630.

Sumitomo, A., Yukitake, H., Hirai, K., Horike, K., Ueta, K., Chung, Y., Warabi, E., Yanagawa, T, Kitaoka, S., Furuyashiki, T., Narumiya, S., Hirano, T., Niwa, M., Sibille, E., Hikida, T., Sakurai, T., Ishizuka, K., Sawa, A., and Tomoda, T. (2018a). Ulk2 controls cortical excitatory-inhibitory balance via autophagic regulation of p62 and GABAA receptor trafficking in pyramidal neurons. Hum. Mol. Genet. doi: 10.1093/hmg/ddy219.

Sumitomo, A., Horike, K., Hirai, K., Butcher, N., Boot, E., Sakurai, T., Nucifora, F.C. Jr., Bassett, A.S., Sawa, A., and Tomoda, T. (2018b). A mouse model of 22q11.2 deletions: Molecular and behavioral signatures of Parkinson's disease and schizophrenia. Sci. Adv. *4*, eaar6637.

Swerdlow, N.R., Braff, D.L., and Geyer, M.A. (2016). Sensorimotor gating of the startle reflex: what we said 25 years ago, what has happened since then, and what comes next. J. Psychopharmacol. *30*, 1072–1081.

Takahashi, N., Sakurai, T., Bozdagi-Gunal, O., Dorr, N.P., Moy, J., Krug, L., Gama-Sosa, M., Elder, G.A., Koch, R.J., Walker, R.H., Hof, P.R., Davis, K.L., and Buxbaum, J.D. (2011). Increased expression of receptor phosphotyrosine phosphatase-β/ζ is associated with molecular, cellular, behavioral and cognitive schizophrenia phenotypes. Transl Psychiatry *1*, e8.

Tang, G., Gudsnuk, K., Kuo, S.H., Cotrina, M.L., Rosoklija, G., Sosunov, A., Sonders, M.S., Kanter, E., Castagna, C., Yamamoto, A., Yue, Z., Arancio, O., Peterson, B.S., Champagne, F., Dwork, A.J., Goldman, J., and Sulzer, D. (2014). Loss of mTOR-dependent macroautophagy causes autistic-like synaptic pruning deficits. Neuron *83*, 1131–1143.

Tripp, A., Oh, H., Guilloux, J.P., Martinowich, K., Lewis, D.A., and Sibille, E. (2012). Brain-derived neurotrophic factor signaling and subgenual anterior cingulate cortex dysfunction in major depressive disorder. Am. J. Psychiatry *169*, 1194–1202.

Vilchez,, D., Saez, I., and Dillin, A. (2014). The role of protein clearance mechanisms in organismal ageing and age-related diseases. Nat. Commun. *5*, 5659.

FIGURE LEGENDS

Figure 1. BDNF regulates autophagy and p62 protein levels in cortical pyramidal neurons

(A) Primary cortical neurons prepared from GFP-LC3 mice were treated with BDNF (100 ng/ml) or vehicle for 30 min, and the fluorescence intensities of GFP+ autophagosomes and their size were scored from > 50 GFP+ puncta per condition. Scale bar, 20 μm. *p<0.05 (Kruskal-Wallis test)

(B) Autophagy flux assay: primary cortical neurons were treated with BDNF (100 ng/ml) for the indicated times in the presence or absence of lysosomal protease inhibitor (bafilomycin A1 [BafA1], 5 ng/ml) and the cell lysates were analyzed by Western blot using LC3 antibody. *p<0.05, **p<0.01 (Kruskal-Wallis test)

(C) Primary cortical neurons prepared from wild-type mice were transfected with GFP-LC3 and treated with BDNF (100 ng/ml) for 30 min. LysoTracker uptake was evaluated to measure acidity of the lysosome in culture. Scale bar, 20 μm. Dotted areas were magnified below. Arrows indicate GFP+ autophagosomes located in the neurite. *p< 0.05 (Kruskal-Wallis test)

(D, E) The PFC (layer 2/3) of *Bdnf*$^{+/-}$ mice (n = 4) and their WT littermates (n = 4) (2 to 2.5

months of age) were immunostained with p62 and CaMKII antibodies, and p62 fluorescence intensities in CaMKII+ neurons were scored and plotted in (E). Scale bar, 20 μm. *p<0.05 (Kruskal-Wallis test)

(F) Quantitative PCR analysis of autophagy-related genes expressed in the PFC of WT (n = 3) and *Bdnf*$^{+/-}$ mice (n = 3) (2 months of age). *p<0.05, **p<0.01 (Kruskal-Wallis test)

Figure 2. Decreased surface presentation of α5GABA$_A$R and behavioral deficits in *Bdnf*$^{+/-}$ mice are rescued by reducing *p62* gene dosage

(A) Surface biotinylation of primary cortical neurons prepared from WT, *Bdnf*$^{+/-}$, or *Bdnf*$^{+/-}$;*p62*$^{+/-}$ mice, analyzed by Western blot using the indicated antibodies. Surface levels of expression were normalized by the total levels of expression for each genotype. The assays were performed in triplicate. *p<0.05 (Kruskal-Wallis test)

(B) BS3 cross-linking assays using the PFC extracts from WT, *Bdnf*$^{+/-}$, or *Bdnf*$^{+/-}$;*p62*$^{+/-}$ mice. Levels of non-crosslinked α5GABA$_A$R (~50 kDa) were normalized by levels of αTubulin at each time point. Differences in the levels of non-crosslinked α5GABA$_A$R at a given time point vs. those of the control sample (No Xlink: no cross-linker added) represent the amount of

surface α5GABA$_A$R that underwent mobility shift toward a higher molecular weight range due to covalent crosslinking with anonymous cell surface proteins. *p<0.05 (Kruskal-Wallis test)

(C) The amplitude of startle response and the percentage of PPI were evaluated for WT (n = 10), *Bdnf*$^{+/-}$ (n = 10), and *Bdnf*$^{+/-}$;*p62*$^{+/-}$ mice (n = 10). No significant difference in startle response ($F_{2,27}$ = 0.378, P = 0.9243, one-way ANOVA). Statistical significance for %PPI; $F_{2,27}$ = 9.775, P < 0.001 (two-way ANOVA with repeated measures); *p<0.05 (Bonferroni post-hoc test).

(D) Schematic diagram of the rule shift assay: Mice were habituated to food, feeding apparatus, different odor cues (O1, O2, etc.; *e.g.*, coriander vs. garlic powder) and texture cues (TA, TB, etc.; *e.g.*, fine vs. coarse digging media) prior to testing, and then food-deprived a day before the assays. Mice were initially trained in a sequence of trials to associate a food reward with a specific stimulus (*i.e.*, either an odor or a digging medium; a stimulus associated with food reward is shown in red). A varying combination of stimulus and food reward was presented to mice per trial. Eight consecutive correct responses to the food reward were considered reaching criterion (*i.e.*, successful establishment of association between the stimulus and the

food reward), and the number of trials to reach criterion were scored for each mouse tested, before and after rule shifting (*e.g.*, from an odor cue to a different texture cue to predict reward).

(E) Numbers of trials to criterion were scored for WT (n = 6), *Bdnf*$^{+/-}$ (n = 6), and *Bdnf*$^{+/-}$;*p62*$^{+/-}$ mice (n = 6) during the initial association phase, as well as the rule shift phase of the assays. No significant difference during the initial association phase ($F_{2,15}$ = 1.25, P = 0.934). Statistical significance during the rule shift phase: $F_{2,15}$ = 9.93, P < 0.001 (one-way ANOVA); **p<0.01 (Bonferroni post-hoc test).

Figure 3. Elevated p62 expression is sufficient to cause downregulation of surface α5GABA$_A$R expression and behavioral deficits

(A) Generation of CaMKII-p62-transgenic mouse lines. Among 3 lines established, 2 lines (#1, #3) showed ~60% higher levels of p62 protein expression in the PFC when compared with WT, whereas the line #2 showed no apparent increase in p62 expression. *p<0.05 (Kruskal-Wallis test)

(B) BS3 cross-linking assays using the PFC extracts from WT, p62-Tg#1 and Tg#2 mice.

Levels of non-crosslinked α5GABA$_A$R (~50 kDa) were normalized by levels of αTubulin at each time point. *p<0.05 (Kruskal-Wallis test)

(C) The amplitude of startle response and the percentage of PPI were evaluated for WT (n = 10), p62-Tg#1 (n = 10), p62-Tg#2 (n = 10), and p62-Tg#3 mice (n = 10). No significant difference in startle response ($F_{3,36}$ = 0.726, P = 0.7121, one-way ANOVA). Statistical significance for %PPI; $F_{3,36}$ = 12.474, P < 0.001 (two-way ANOVA with repeated measures); *p<0.05 (Bonferroni post-hoc test).

(D) Numbers of trials to criterion were scored for WT (n = 7), p62-Tg#1 (n = 7), and p62-Tg#3 mice (n = 8) during the initial association phase, as well as the rule shift phase of the assays. No significant difference during the initial association phase ($F_{2,19}$ = 1.968, P = 0.936). Statistical significance during the rule shift phase: $F_{2,19}$ = 12.56, P < 0.001 (one-way ANOVA); **p< 0.01 (Bonferroni post-hoc test).

Figure 4. Gene expression profiling with human postmortem brains suggest altered autophagy machinery in MDD

(A) Expression levels of the autophagy-enhancing genes (95 genes, **Supplemental Table 1**) vs.

the autophagy-attenuating genes (38 genes, **Supplemental Table 2**) in the corticolimbic area of the MDD brain cohorts were compared with those of the control cohorts. Overall expression levels of the autophagy-attenuating genes in MDD, as represented by the area under the curve (AUC = 0.60) were significantly different from those of the autophagy-enhancing genes, as represented by the AUC (= 0.44) ($p<0.01$).

(B) The autophagy-attenuating genes in MDD tend to cluster toward the direction of upregulation, whereas the autophagy-enhancing genes in MDD tend to cluster toward the direction of downregulation. As internal reference, the ranking of *BDNF* and *Somatostatin* (*SST*) were plotted, both of which have been reported to be significantly downregulated in the corticolimbic area of the MDD brains (Ding et al., 2015), as represented by the AUC values of 0.0035 and 0.031, respectively.

Figure 5. Two modes of mechanisms underlying GABA dysfunction following reduced BDNF signaling

Attenuated BDNF expression or signaling in the cortical pyramidal neurons, due to chronic stress or other neuropsychiatric insults, leads to GABA dysfunction through transcriptional

suppression of GABA synapse genes in neighboring inhibitory neurons (paracrine mode) (Oh et al., 2016) and also via reduced surface presentation of α5GABA$_A$R in the pyramidal neurons (autocrine mode) (this study), together contributing to cognitive and other behavioral deficits relevant to neuropsychiatric disorders, including MDD.

Supplemental Figure 1. Surface presentation of α1- and α2-GABA$_A$R in *Bdnf*$^{+/-}$ mice

BS3 cross-linking assays using the PFC extracts from WT (n=3) and *Bdnf*$^{+/-}$ mice (n=3). Levels of non-crosslinked α1- and α2-GABA$_A$R (~50 kDa) were normalized by levels of αTubulin at each time point. Differences in the levels of non-crosslinked α1- or α2-GABA$_A$R at a given time point vs. those of the control sample (No Xlink: no cross-linker added) represent the amounts of surface GABA$_A$R that underwent mobility shift toward a higher molecular weight range due to covalent crosslinking with anonymous cell surface proteins. No significant differences in the surface levels of α1- and α2-GABA$_A$R were observed in the PFC of WT vs. *Bdnf*$^{+/-}$ mice.

Figure 1

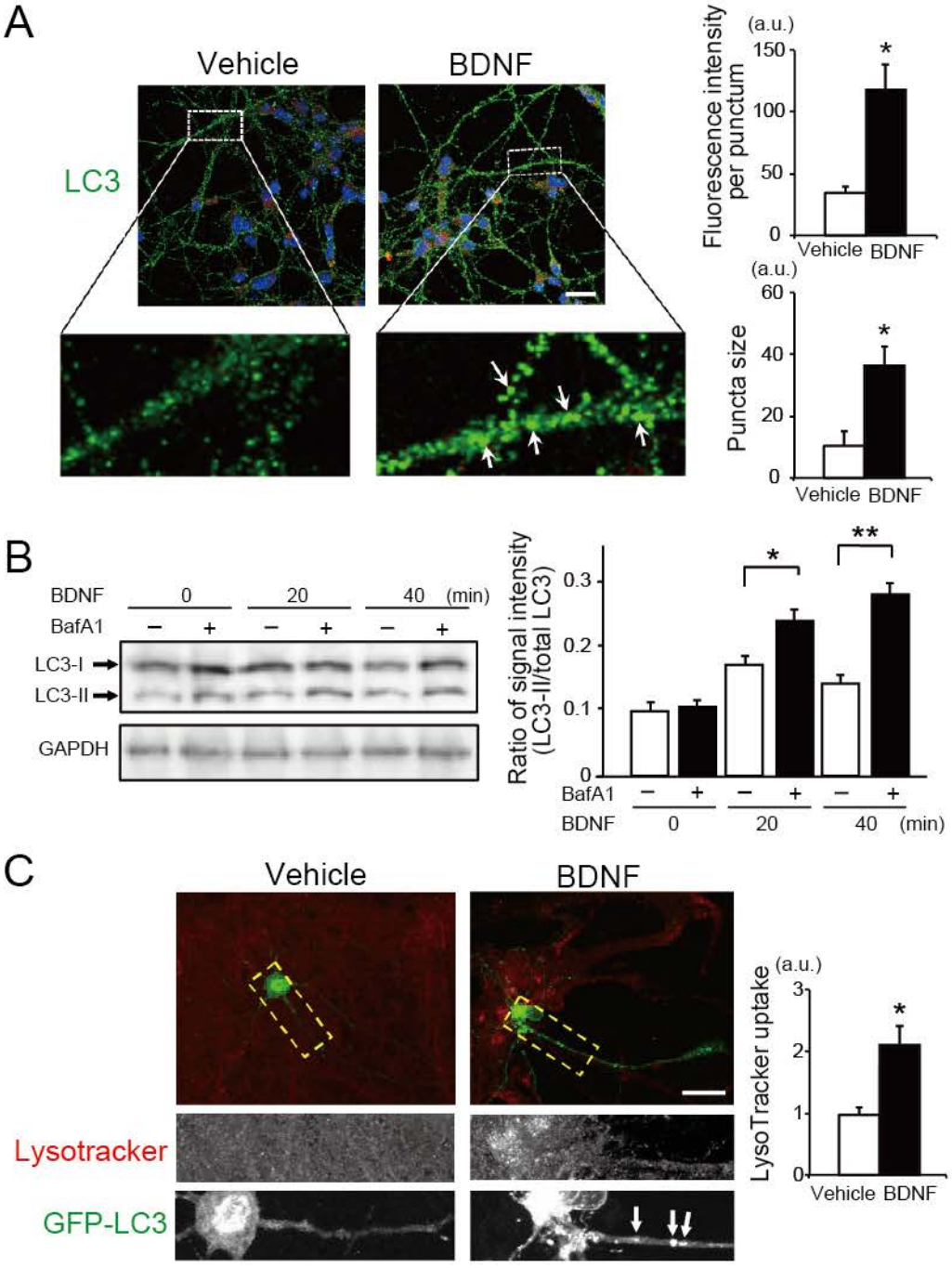
A
Vehicle
BDNF
LC3
Fluorescence intensity per punctum
(a.u.)
150
100
50
0
Vehicle BDNF
Puncta size
(a.u.)
60
40
20
0
Vehicle BDNF
B
BDNF 0 20 40 (min)
BafA1 − + − + − +
LC3-I
LC3-II
GAPDH
Ratio of signal intensity (LC3-II/total LC3)
0.3
0.2
0.1
0
BafA1 − + − + − +
BDNF 0 20 40 (min)
C
Vehicle
BDNF
Lysotracker
GFP-LC3
LysoTracker uptake
(a.u.)
3
2
1
0
Vehicle BDNF

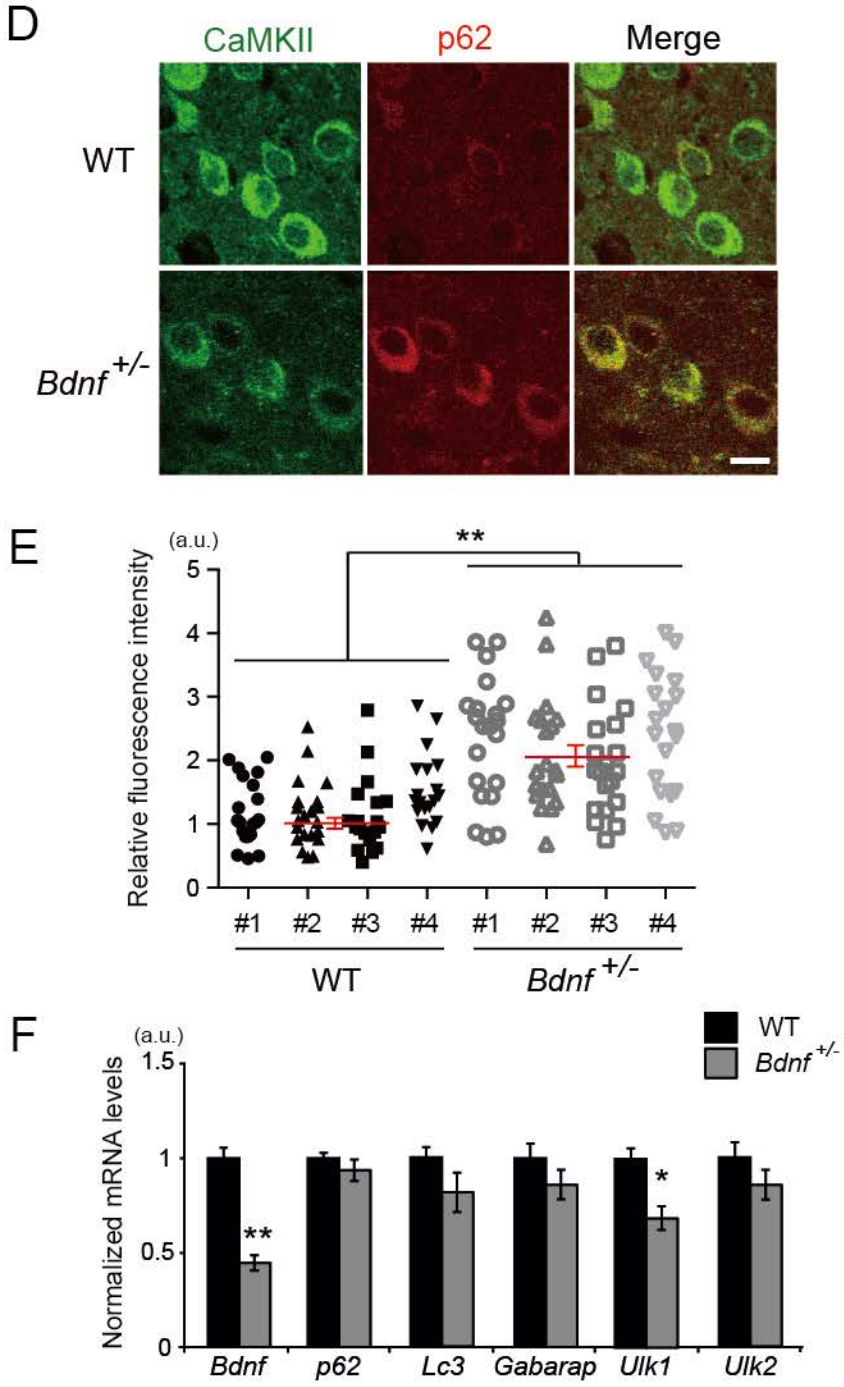
D
CaMKII
p62
Merge
WT
Bdnf +/-
E
Relative fluorescence intensity
(a.u.)
5
4
3
2
1
0
#1 #2 #3 #4 #1 #2 #3 #4
WT
Bdnf +/-
F
WT
Bdnf +/-
Normalized mRNA levels
(a.u.)
1.5
1
0.5
0
Bdnf p62 Lc3 Gabarap Ulk1 Ulk2

Figure 2

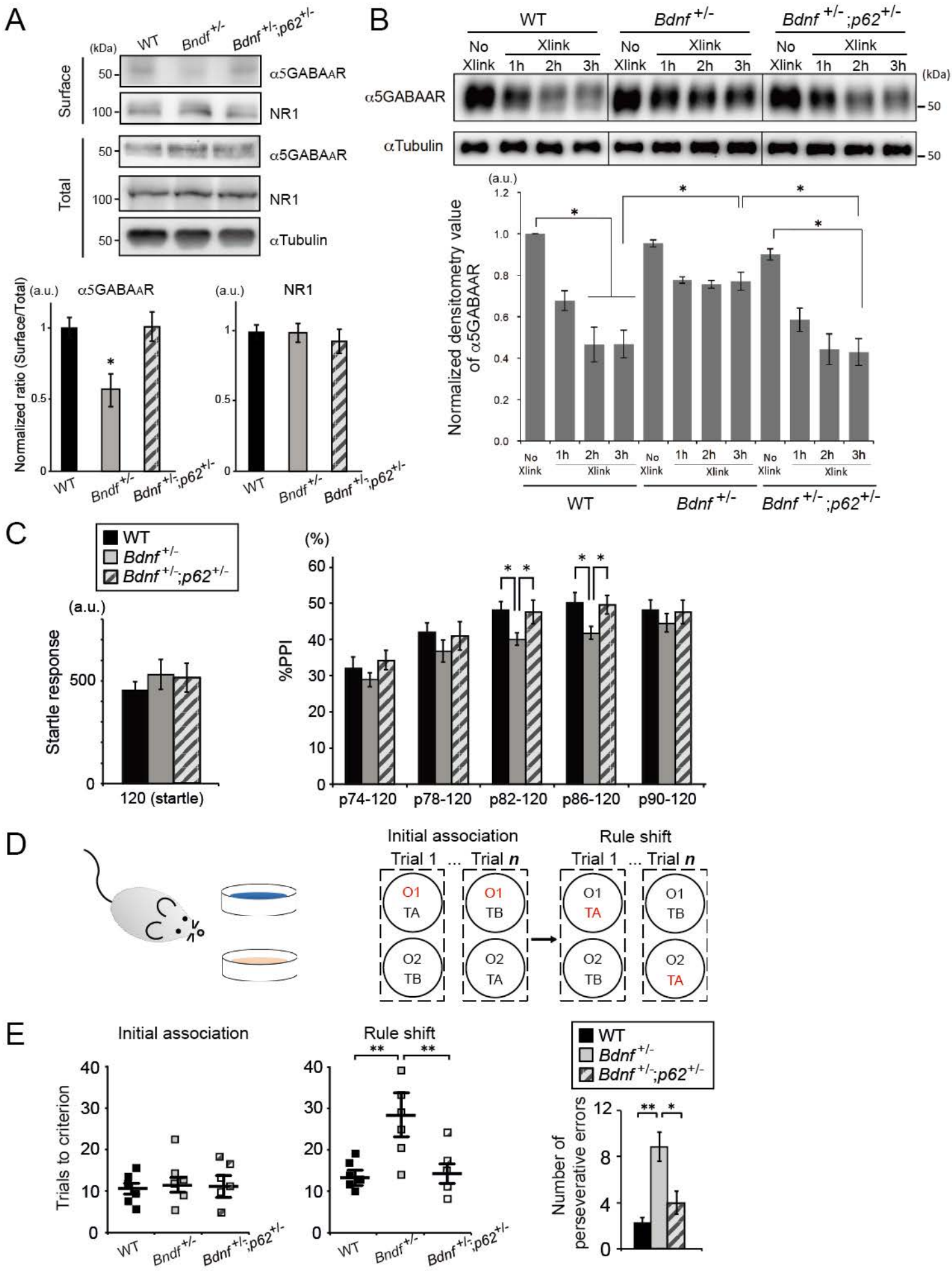
A
(kDa)
WT
Bndf+/-
Bndf+/-;p62+/-
Surface
Total
50
100
α5GABAAR
NR1
αTubulin
Normalized ratio (Surface/Total)
(a.u.)
B
No Xlink
Xlink
1h
2h
3h
α5GABAAR
αTubulin
Normalized densitometry value of α5GABAAR
C
Startle response
120 (startle)
%PPI
p74-120
p78-120
p82-120
p86-120
p90-120
D
Initial association
Rule shift
Trial 1
Trial n
O1
O2
TA
TB
E
Initial association
Rule shift
Trials to criterion
Number of perseverative errors

Figure 3

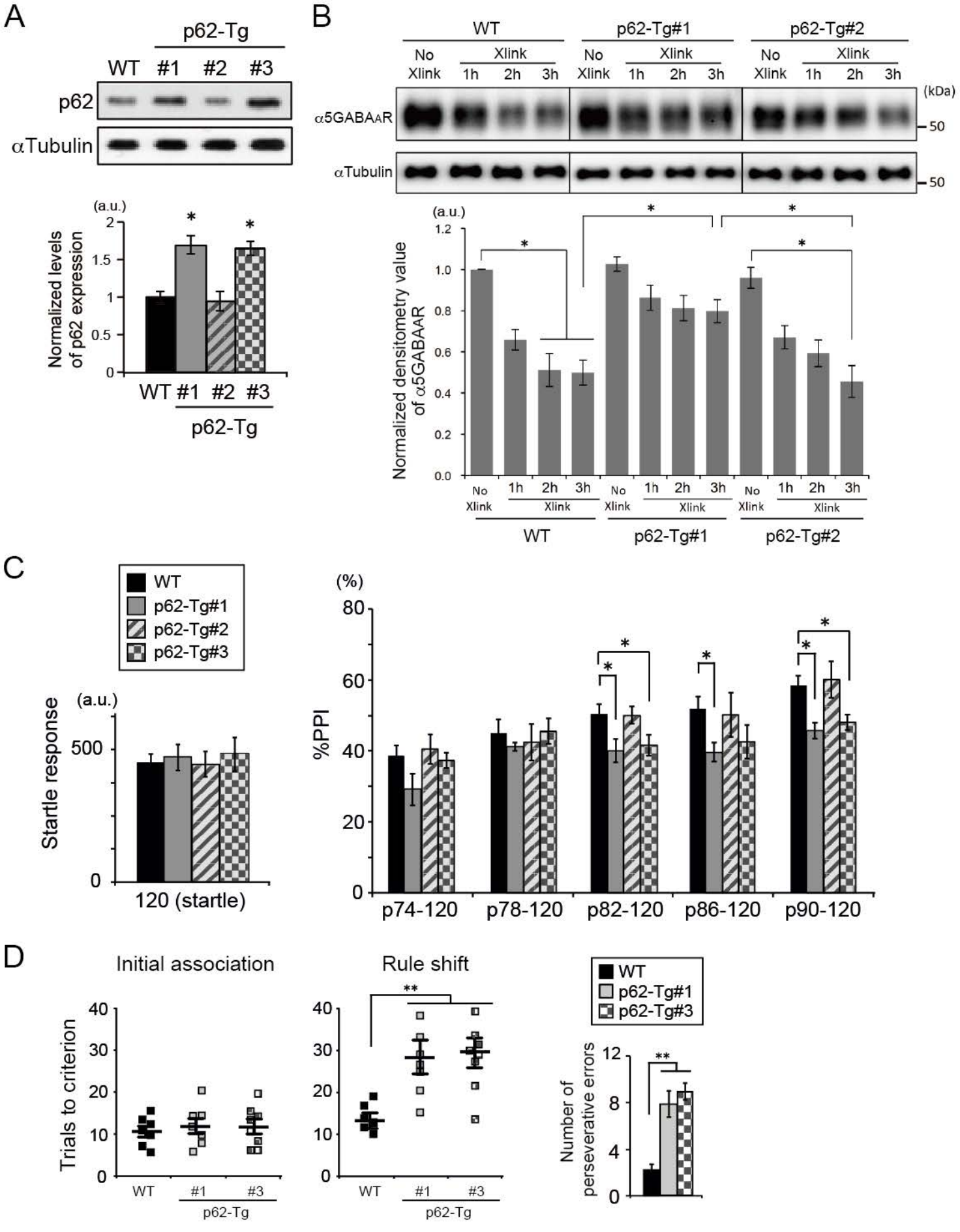
A
p62-Tg
WT #1 #2 #3
p62
αTubulin
(a.u.)
Normalized levels of p62 expression
WT #1 #2 #3
p62-Tg
B
WT
p62-Tg#1
p62-Tg#2
No Xlink
Xlink 1h 2h 3h
α5GABAAR
αTubulin
(kDa)
50
Normalized densitometry value of α5GABAAR
C
WT
p62-Tg#1
p62-Tg#2
p62-Tg#3
Startle response
120 (startle)
%PPI
p74-120
p78-120
p82-120
p86-120
p90-120
D
Initial association
Rule shift
Trials to criterion
Number of perseverative errors

Figure 4

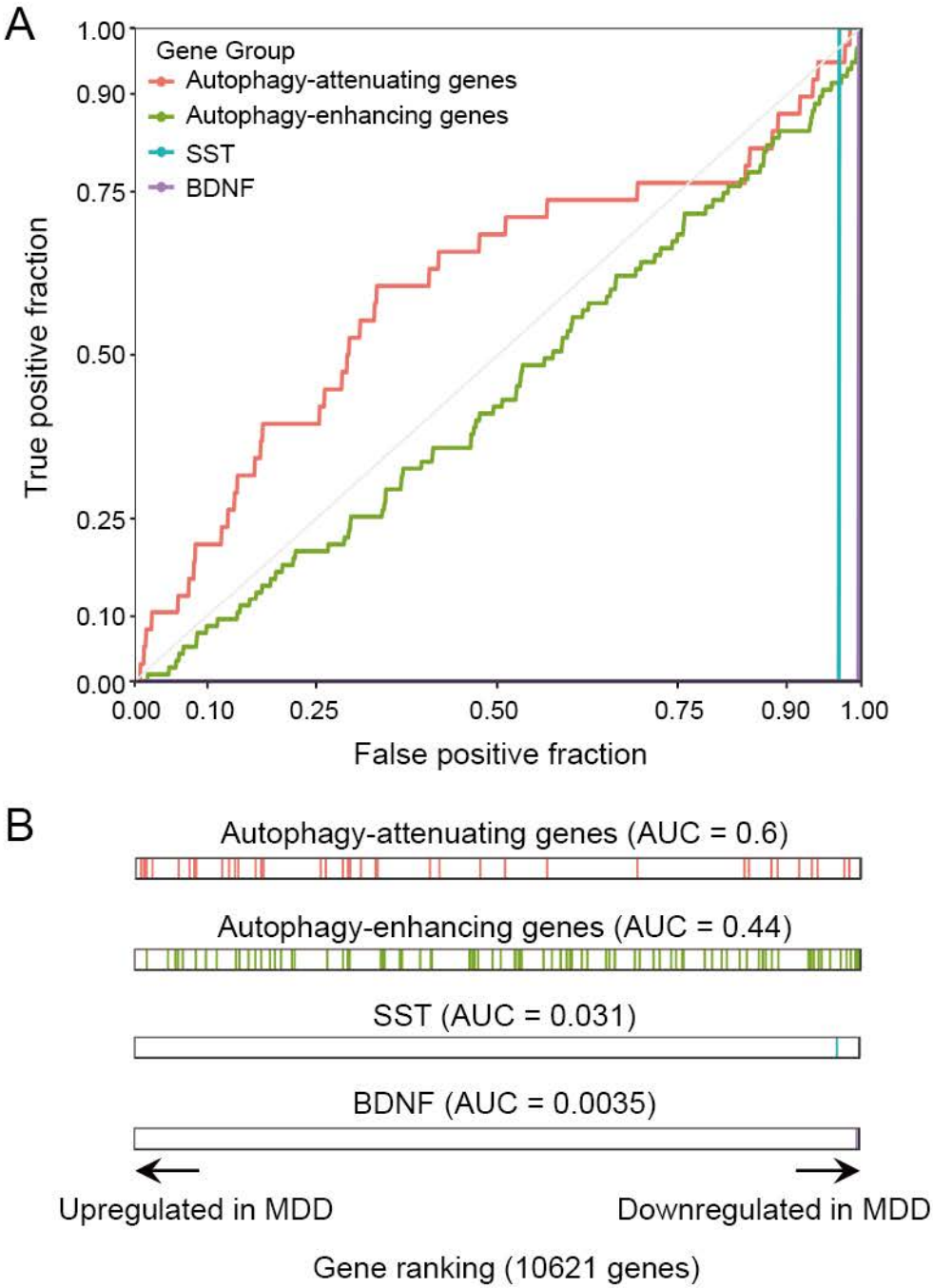
A
Gene Group
Autophagy-attenuating genes
Autophagy-enhancing genes
SST
BDNF
True positive fraction
False positive fraction
1.00
0.90
0.75
0.50
0.25
0.10
0.00
0.00
0.10
0.25
0.50
0.75
0.90
1.00
B
Autophagy-attenuating genes (AUC = 0.6)
Autophagy-enhancing genes (AUC = 0.44)
SST (AUC = 0.031)
BDNF (AUC = 0.0035)
Upregulated in MDD
Downregulated in MDD
Gene ranking (10621 genes)

Figure 5

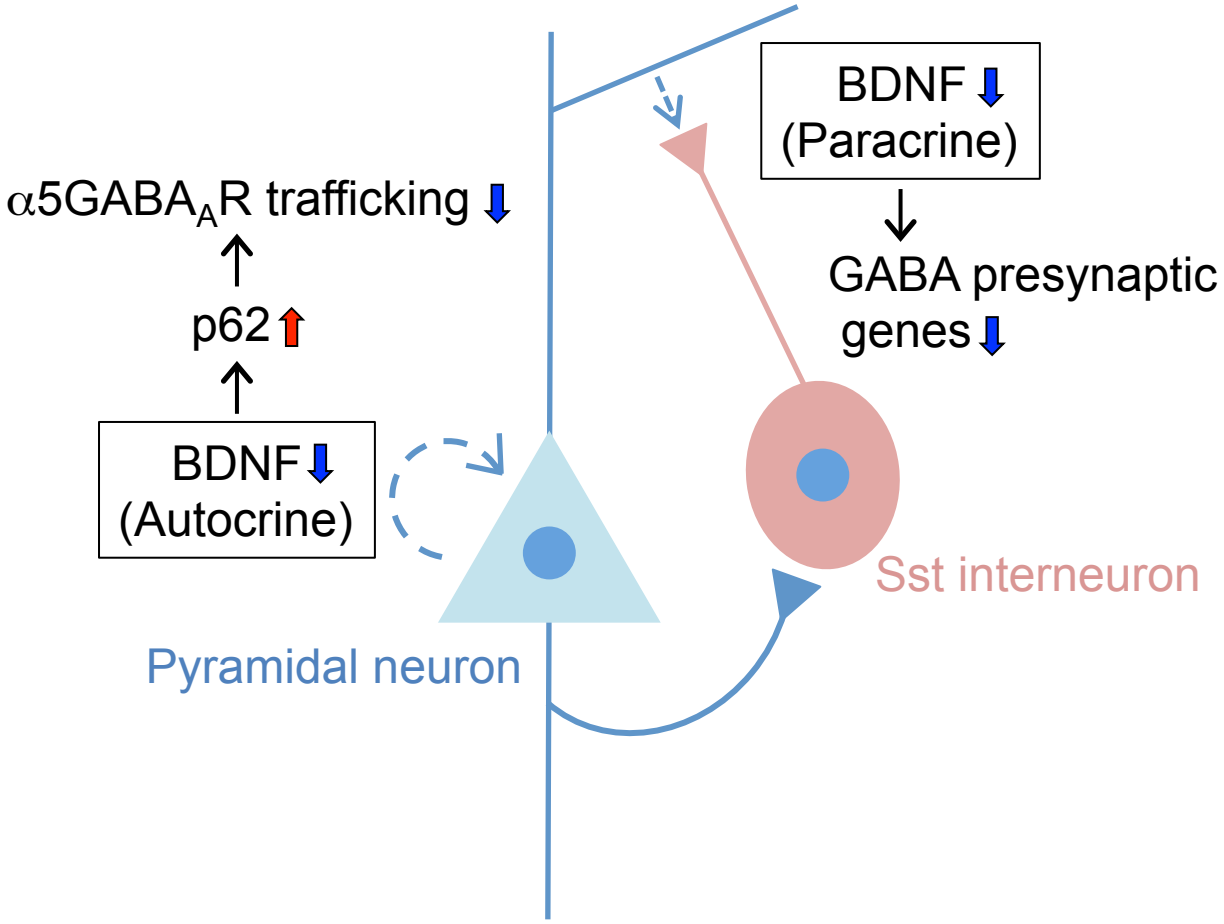
BDNF ⬇
(Paracrine)
↓
GABA presynaptic genes ⬇
α5GABA$_A$R trafficking ⬇
↑
p62 ⬆
↑
BDNF ⬇
(Autocrine)
Sst interneuron
Pyramidal neuron

Supplementary Figure 1

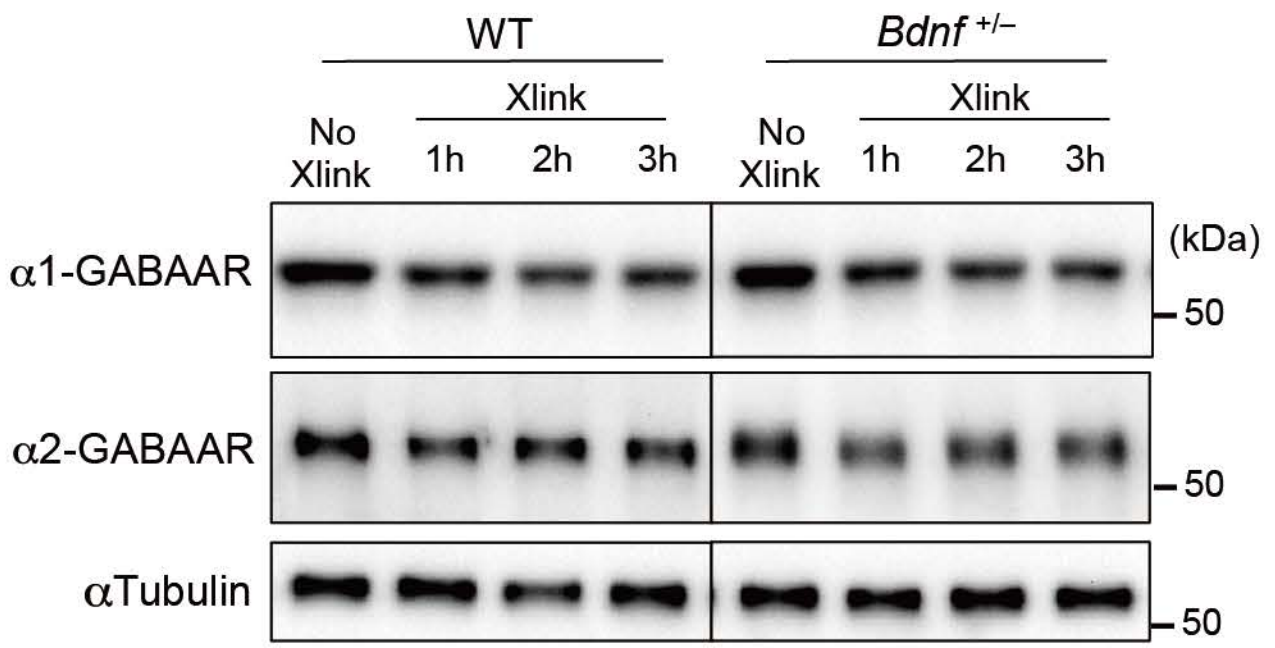

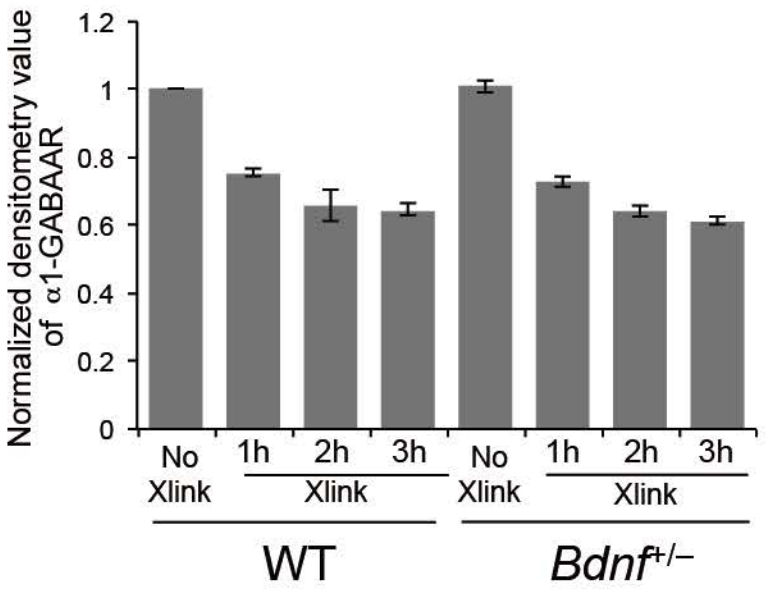

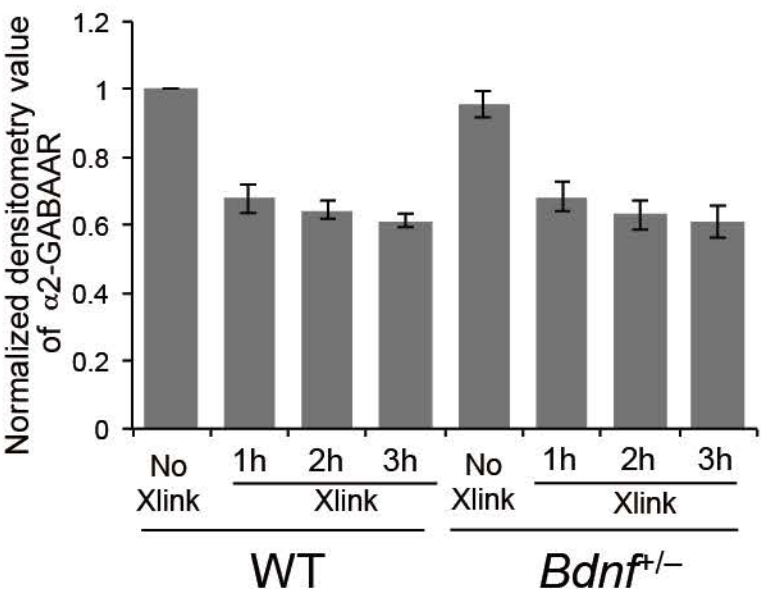

Supplementary Table 1

Supplementary Table 1. Customized list of the autophagy-enhancing genes

gene_symbol	p_value_aw	medianEffect
EIF2AK4	0.034984747	1.162669369
TRIM8	0.117535166	0.818133331
SMCR8	0.152032012	1.27782292
DAPK1	0.155987666	0.770628523
ATPIF1	0.173100273	1.553535083
FYCO1	0.22174155	0.700398633
AMBRA1	0.222481311	0.855662055
SUPT5H	0.2542512	0.887141728
SESN2	0.296281612	0.289254212
LRRK2	0.310434987	0.724924336
TICAM1	0.366607476	0.621448164
SH3BP4	0.382627436	0.474681386
FOXO1	0.417930421	0.719989416
PIP4K2B	0.441107052	0.897350304
MAPK3	0.457994539	0.776615843
SIRT1	0.489636852	0.84425061
TP53INP2	0.510219565	0.603880019
MID2	0.531684964	1.165562608
PRKAA2	0.570616138	0.071009746
KIAA1324	0.720906977	1.158383241
PIP4K2C	0.740623576	0.098748746
CLEC16A	0.769017701	0.366000548
KDR	0.829098108	0.950940013
TPCN1	0.838233782	0.105844955
RALB	0.879007721	0.559178164
RAB3GAP1	0.87990999	0.227513656
HDAC6	0.88163092	0.698590534
WAC	0.932930515	0.284368044
MFN2	0.960825911	0.012070394
SPTLC2	0.9638599	0.138458922
OPTN	0.934316825	−0.158996104
MTDH	0.926198663	−0.158968805
CALCOCO2	0.920138405	−0.693186218
HTRA2	0.912784201	−0.097381324
SCOC	0.875743904	−0.130406807
TBK1	0.851887581	−0.067948212
PAFAH1B2	0.815563412	−0.308292491
HIF1A	0.814421523	−0.266228513

gene_symbol	p_value_aw	medianEffect
UVRAG	0.807666792	−0.352264888
VPS13C	0.805675172	−0.420452464
BECN1	0.801819885	−0.411825619
DHRSX	0.744477639	−0.199340534
FBXO7	0.722127389	−0.037960469
TFEB	0.700580266	−0.018485743
CAMKK2	0.684909236	−1.566969409
RAB12	0.675408813	−0.942742606
PARK7	0.670962621	−0.143228124
TRIM22	0.645755579	−0.257948582
BNIP3L	0.63394445	−0.458369868
RIPK2	0.584106581	−0.575034615
STK11	0.564148668	−1.371998267
TSC1	0.56266651	−0.381984843
BNIP3	0.497204595	−0.535210457
PLK2	0.463951888	−0.532009937
PIK3CB	0.448217588	−1.412430676
FLCN	0.412448545	−0.97800392
TRIM13	0.397255626	−0.012605542
PLEKHF1	0.394280388	−0.76786282
EPM2A	0.322975238	−0.639018648
TSC2	0.300476697	−0.370809509
PRKAA1	0.286510875	−1.267519244
PIM2	0.240186706	−0.754203311
SH3GLB1	0.203863007	−1.221496301
SPTLC1	0.194087845	−1.544333353
LARP1	0.180830995	−0.861198852
MAP3K7	0.099798795	−0.823531047
LRSAM1	0.096247717	−1.217880954
C9orf72	0.092959608	−1.288356398
GSK3B	0.077148197	−1.615224996
TMEM59	0.070357029	−0.926792913
CDC37	0.051240185	−1.009629071
PINK1	0.029979192	−1.11375343
IKBKG	0.01017456	−1.031605376
PRKD1	0.003644101	−1.210506542
BAD	0.00279823	−1.347739423
DCN	0.00053366	−1.634289599

Supplementary Table 2. Customized list of the autophagy maturation genes

gene_symbol	p_value_aw	medianEffect
SNX14	0.147074663	0.675692116
VPS33A	0.672570756	0.904040607
SNAP29	0.74007777	0.125522767
VCP	0.834424819	0.401512237
VPS16	0.83737859	0.519108401
LIX1	0.932354581	−0.273249391
CALCOCO2	0.920138405	−0.693186218
UVRAG	0.807666792	−0.352264888
LAMP2	0.702094436	−0.388714965
GABARAPL2	0.575407589	−0.584347403
CLN3	0.50934347	−0.764568165
STX17	0.423380567	−0.528784357
GABARAP	0.398240467	−0.204459714
VAMP8	0.343637134	−0.585788979
TSG101	0.259045476	−0.850928386
SNAPIN	0.212957443	−0.864722301
TBC1D25	0.202719141	−0.681825632
MCOLN1	0.166698522	−0.248693735
MAP1LC3A	0.087320874	−1.023047875
PHF23	0.079421335	−0.608212865
UBQLN1	0.018410413	−1.477666864
LIX1L	0.001097072	−1.922553403

Supplementary Table 3. Customized list of the autophagy-attenuating genes

gene_symbol	p_value_aw	medianEffect
EIF4G1	0.015020149	1.437745811
KIF25	0.023130496	1.190166014
DAP	0.030276057	0.770542156
AKT1	0.055029187	1.326819928
SIRT2	0.197292157	1.515489055
UBQLN4	0.213909236	0.844394059
GOLGA2	0.219871575	1.017417495
WDR6	0.340445438	0.364700969
CHMP4A	0.35986216	1.067377846
MT3	0.37116458	0.599926824
MTM1	0.439070332	0.047310997
TBC1D14	0.454628943	0.909881069
CTSA	0.461122681	0.417650653
CHMP4B	0.648297053	0.468667816
BCL2	0.663554844	0.959336518
PIK3CA	0.715826288	0.757406388
RASIP1	0.739175407	0.225829356
TSPO	0.812726674	0.137934588
SCFD1	0.817457961	0.658080788
QSOX1	0.955435835	0.180495981
NPC1	0.97898503	0.774296622
TLK2	0.910991997	−0.218861268
LARS	0.841193673	−0.339605394
NRBP2	0.735582054	−0.206637359
RNF5	0.504352321	−0.048494504
HERC1	0.235670276	−1.184952443
RNF41	0.167279729	−1.393432626
LZTS1	0.120550042	−1.481081734
RRAGA	0.090564919	−0.559871294
PHF23	0.079421335	−0.608212865
POLDIP2	0.022472272	−1.070552502